

Review

Damage Characteristics of Thermally Deteriorated Carbonate Rocks: A Review

Umer Waqas ^{1,*}, Hafiz Muhammad Awais Rashid ¹, Muhammad Farooq Ahmed ¹, Ali Murtaza Rasool ²
and Mohamed Ezzat Al-Atroush ^{3,*}

¹ Department of Geological Engineering, University of Engineering and Technology, Lahore 54890, Pakistan; awais.rashid@uet.edu.pk (H.M.A.R.); mfageo@uet.edu.pk (M.F.A.)

² National Engineering Services Pakistan (NESPAK), Lahore 54700, Pakistan; ali_eng@hotmail.com

³ Department of Engineering Management, College of Engineering, Prince Sultan University, Riyadh 11543, Saudi Arabia

* Correspondence: umerwaqas@uet.edu.pk (U.W.); mezzat@psu.edu.sa (M.E.A.-A.)

Abstract: This review paper summarizes the recent and past experimental findings to evaluate the damage characteristics of carbonate rocks subjected to thermal treatment (20–1500 °C). The outcomes of published studies show that the degree of thermal damage in the post-heated carbonate rocks is attributed to their rock fabric, microstructural patterns, mineral composition, texture, grain cementations, particle orientations, and grain contact surface area. The expressive variations in the engineering properties of these rocks subjected to the temperature (>500 °C) are the results of chemical processes (hydration, dehydration, deionization, melting, mineral phase transformation, etc.), intercrystalline and intergranular thermal cracking, the separation between cemented particles, removal of bonding agents, and internal defects. Thermally deteriorated carbonate rocks experience a significant reduction in their fracture toughness, static–dynamic strength, static–dynamic elastic moduli, wave velocities, and thermal transport properties, whereas their porous network properties appreciate with the temperature. The stress–strain curves illustrate that post-heated carbonate rocks show brittleness below a temperature of 400 °C, brittle–ductile transformation at a temperature range of 400 to 500 °C, and ductile behavior beyond this critical temperature. The aspects discussed in this review comprehensively describe the damage mechanism of thermally exploited carbonate rocks that can be used as a reference in rock mass classification, sub-surface investigation, and geotechnical site characterization.

Keywords: mineral dilatancy; thermal cracking; static–dynamic compression; brittle–ductile transition; thermal transport properties



Citation: Waqas, U.; Rashid, H.M.A.; Ahmed, M.F.; Rasool, A.M.; Al-Atroush, M.E. Damage Characteristics of Thermally Deteriorated Carbonate Rocks: A Review. *Appl. Sci.* **2022**, *12*, 2752. <https://doi.org/10.3390/app12052752>

Academic Editor: Fernando Rocha

Received: 14 January 2022

Accepted: 27 February 2022

Published: 7 March 2022

Publisher's Note: MDPI stays neutral with regard to jurisdictional claims in published maps and institutional affiliations.



Copyright: © 2022 by the authors. Licensee MDPI, Basel, Switzerland. This article is an open access article distributed under the terms and conditions of the Creative Commons Attribution (CC BY) license (<https://creativecommons.org/licenses/by/4.0/>).

1. Introduction

Earthen materials such as rocks have a wide range of applications in various rock-engineering related domains, including rock slope stabilization, rock drilling, tunneling and excavation, coal gasification, nuclear waste repositories, geothermal energy extraction, construction material, and foundation engineering [1–4]. Rocks are heterogeneous, anisotropic, and aggregate of different minerals. They are not perfectly elastic material but rather brittle in nature. However, deep-seated rocks show ductility under high pressure and temperature conditions [5]. The rock mass exposed to the surface is found discontinuous due to its weathering. Temperature is one of the most important weathering agents that significantly alter the engineering properties of the rock mass. Construction of sensitive structures, such as skyscrapers, dams, nuclear power plants, tunnels, etc., in the thermally deteriorated rock mass is taken into account as a major challenge. These structures may experience severe damage or reduction in their service life under the adverse effects of altered engineering properties of the thermally damaged rock mass [6]. Therefore, the study of thermal effects on rock properties has been garnering attention for the last few decades.

Carbonate rocks are a sub-class of sedimentary rocks and abundantly found on the upper Earth's crust. Limestone and dolostone are the two major types of carbonate rocks and have a wide range of applications in the construction, cement, glass, mining, and petroleum industries [7]. Several researchers have investigated the engineering behavior of carbonate rocks subjected to various temperature ranges between ambient temperature and high temperature (20–1000 °C) [6–13]. They have noticed that limestone and dolostone under high temperatures experience mineralogical alteration, inter-granular and intra-granular cracking, reduction in dynamic–mechanical strength parameters, and appreciation in porosity and permeability.

In high-temperature rock mechanics and geotechnics, the evaluation of the engineering characteristics of carbonate rocks is of great interest. For example, dimension stones obtained from carbonate or silicate rocks are important construction materials. In a building fire event, their temperature may rise above 800 °C [14]. The underground coal gasification process may increase the temperature of host carbonate rocks up to 1500 °C [15]. This process not only significantly damages host rocks but also releases oxides of nitrogen, carbon, sulfur, etc., in the environment. Similarly, during a plate tectonic event (at depth > 40 km and 500–850 °C), thick deposits of carbonate rocks at the subduction zone liberate excessive carbon dioxide, which is one of the major global warming factors [16]. Furthermore, magmatic activities, such as contact metamorphism, increase the temperature of country rocks from 300 to 800 °C [17]. At a shallow depth, the decay of radioactive elements in their repositories heats the host rocks from 50 to 250 °C [7]. The level of temperature and pressure increases with depth. Therefore, the extraction of geothermal energy and hydrocarbons from deep-seated carbonate rocks requires special attention because of their altered geomechanical characteristics [18].

This study aims to summarize the research work on thermally treated carbonate rocks to discern their behavior against increasing temperature. In this research work, the literature review covers the experimental findings of pre-heated and post-heated carbonate rocks. Furthermore, it evaluates the damage characteristics of thermally degraded carbonate rocks in terms of mineral dilatancy, rock fabric, microstructural properties, physico-mechanical behavior, fluid transport properties, thermal transport properties, and dynamic response.

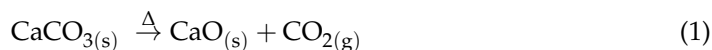
2. Thermal Dilatancy and Alteration in Rock Fabric

Carbonate rocks obtained from various sources can differ significantly in their texture, depositional environment, chemical composition, crystal structure, and mineral geometry [19]. Limestones contain more than 50% calcite and a trace amount of a variety of minerals, including quartz, feldspar, pyrite, siderite, micrite, clay minerals, and other materials. On the other hand, dolostone is composed of the dolomitization process in which calcite transforms into magnesium-rich calcium carbonate. It contains dolomite as a primary mineral and a trivial amount of quartz, mica, iron oxide, and clay minerals [20]. They are chemically reactive substances and show large variations in their chemical reactions. Microstructure patterns and impurities, such as silica, iron, magnesium, manganese, sodium, potassium, etc., considerably affect their chemical reactivity [19]. The calcite and dolomite minerals belong to the hexagonal-rhombohedral crystal system. In this crystal system, the hexagonal unit cell is placed over the rhombohedral unit cell [21]. Calcite mineral has ordered planes of Ca^{2+} attached with the CO_3^{2-} groups orthogonal to the c-axis. Whereas, dolomite mineral exhibits a well-defined order of alternating planes of Ca^{2+} and Mg^{2+} bonded with the CO_3^{2-} groups perpendicular to the c-axis [22].

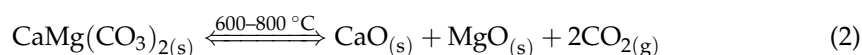
2.1. Thermal Decomposition of Calcite and Dolomite

The investigation of thermal decomposition of the primary carbonate minerals is of great interest. It develops a solid background rationale to anticipate the possible reason behind microstructural variations in carbonate rocks under a thermal environment. The reaction kinetics explains the decomposition of carbonate minerals into their respective constituents at elevated temperatures.

The rate of reaction is controlled by some important factors, such as heat transfer rate, mass transfer rate, or their combination [23]. It is evident from past studies that particle size, crystal structure, the order of atoms in a unit cell, possible impurities, and crystal habit substantially affect the thermal transport mechanism and mineral dilatancy [23,24]. Considerable variations are found in the kinetic parameters of thermally decomposed carbonate minerals. For example, a great discrepancy is reported in the literature regarding the activation energy values of calcite (155–222 kJ mol⁻¹) and dolomite (146–440 kJ mol⁻¹) [25]. As the temperature increases, the calcite starts to deform due to thermal expansion and chemical reactions. It decomposes into calcium oxide (cubic crystal system) with the liberation of carbon dioxide at a temperature greater than 600 °C [26]. Chemically, it can be expressed as follows:



The hexagonal–rhombohedral crystal system of dolomite (i.e., CaMg(CO₃)₂) begins to deform because of the dislocation of cations and anions. Its thermal decomposition produces calcium oxide (cubic crystal system), magnesium oxide (cubic crystal system), and carbon dioxide gas [25]. Several models have been developed to understand the thermal decomposition mechanism for both natural and synthetic dolomites [27–32]. The single-step reaction for the dolomite decomposition is described below:



Another proposed model suggests that the thermal decomposition of a dolomite mineral completes in more than one step [33]. In the first step, it breaks into magnesium carbonate and calcium carbonate. In the second step, unstable magnesium carbonate decomposes into magnesium oxide. Finally, calcium carbonate turns into its respective metallic oxide against increasing temperature.

To study thermal damage characteristics and decomposition of carbonate minerals, several techniques have been utilized, such as thermogravimetric analysis (TGA), differential scanning calorimetry (DSC), differential thermal analysis (DTA), thermo-balance, scanning electron microscopy, optical microscopy, X-ray diffraction, high-temperature X-ray diffraction, etc. [34–48]. A summary of major developments and employed quantitative methods regarding the decomposition of carbonate minerals is provided in Table 1.

Table 1. Summary of major developments regarding the thermal decomposition of primary carbonate minerals.

Mineral Type	Major Developments	Reference
Calcite	The rate of mass loss was studied using isothermal and dynamic methods.	[34]
Calcite	A comparative study was conducted using isothermal–dynamic techniques and thermogravimetric analysis.	[35]
Calcite	Morphological variations were studied in polycrystalline CaCO ₃ under temperature and pressure.	[36]
Dolomite	Thermal decomposition and weight loss analysis was carried out under non-isothermal conditions using in situ X-ray diffraction and thermogravimetry.	[37]
Calcite	Reaction rate constants were determined based on the grain model using thin slab-type pellets.	[38]
Calcite	Thermal decomposition was analyzed using dynamic X-ray diffraction under the effect of steam and CO ₂ .	[39]
Dolomite	Prediction of rate of reaction using stoichiometric analysis and thermogravimetric analysis.	[27]
Calcite	Thermal decomposition was investigated using thermogravimetric analysis subjected to non-isothermal conditions.	[40]

Table 1. Cont.

Mineral Type	Major Developments	Reference
Calcite	The kinetic parameters were obtained from a new method that avoids the Arrhenius equation.	[41]
Dolomite	Thermo-mechanical damage was examined under intensive grinding using X-ray diffraction and thermal analysis.	[42]
Calcite	The solid-state transformation was evaluated using thermogravimetric analysis, evolved gas analysis-mass spectrometry, and high-temperature XRD.	[43]
Dolomite	The thermal decomposition mechanism was explained in detail using thermogravimetry and X-ray powder diffraction.	[33]
Dolomite	Thermal expansion and decomposition behavior were investigated using thermogravimetric analysis, differential thermal analysis, XRD, and scanning electron microscopy.	[29]
Dolomite	Stoichiometric ordered and disordered single crystal dolomite was studied using X-ray diffraction under high pressure and temperature conditions.	[44]
Dolomite	Investigation of kinetics of isothermal and non-isothermal decompositions.	[25]
Calcite	A simulated model was presented that effectively predicted the conversion time curve and described the calcination–carbonation cycle after performing thermogravimetric analysis.	[45]
Dolomite	Differential scanning calorimetry and thermogravimetric analysis based on non-isothermal calcination carried out under varying CO ₂ –air environments.	[46]
Calcite	Thermo-physical decomposition was studied under equilibrium dynamic simulation.	[47]
Calcite	Parameters including unit cell volume alteration, thermal expansion, variations along lattice axis, and thermal strains were studied using high-temperature X-ray powder diffraction.	[26]
Calcite	Thermal decomposition analysis was performed to validate improved reaction kinetic equation based on the pore structure model.	[48]

2.2. Reasons behind the Thermal Expansion

The crystal structure of a dolomite mineral is intermediate between calcite (CaCO₃) and magnesite (MgCO₃). However, it differs from calcite in terms of two aspects: alternating layers of calcium and magnesium in the unit cell and slight tilting of the carbonate group [49]. Thermal expansion of calcite along the a-axis is observed negative. On the other hand, in dolomite, it is measured positively along both the a-axis and c-axis [50]. Single carbonate crystals, such as calcite, show typical strength–temperature behavior (strength decrease with the temperature). Whereas, double carbonate crystals, such as dolomite, exhibit a different behavior that is shown by the calcite. It is attributed to the thermal vibration of the carbonate group that hinders the dislocation movement against increasing temperature [51].

In dolomite, the octahedral system of CaO₆ and MgO₆ plays an important role in stabilizing the crystal structure. The Ca–O bond length is found larger in dolomite as compared to that in calcite [49]. The variations in the bond length of Ca–O relative to temperature is different in both single carbonate crystals and double carbonate crystals. At the temperature range of 24 to 600 °C, in dolomite, a linear elongation in Ca–O bond length is observed at a faster rate. Whereas, in the case of calcite, an exponential trend is noted in the expansion of Ca–O bond length at a slower rate [52]. The bond strength can be expressed in terms of thermal expansion. Longer bonds (in dolomite) show less resistance and expand rapidly. There are different trends reported in the literature that explain the thermal behavior of polyhedral crystals in terms of volume expansion (VE) and quadratic elongation (QE). In dolomite, Ca-octahedron shows a very slight or no change in QE. Whereas, in Mg-octahedron, QE increases substantially. This behavior shows a contrast with the QE trends observed in calcite and magnesite. The QE under increasing temperature varies sharply for Ca-octahedron but, in the case of Mg-octahedron, exhibits

no distortion [52,53]. The possible reason for such trends in these carbonate minerals is the thermal expansion between the oxygen atoms of octahedra at the basal edge and lateral edge. Furthermore, the Ca-octahedron of calcite shows less anisotropic thermal expansion. However, the thermal expansion in Mg-octahedron of dolomite displays more anisotropic character relative to magnesite [54]. Figure 1 illustrates the thermal effect on the interatomic distances of Ca-O and Mg-O in calcite, dolomite, and magnesite.

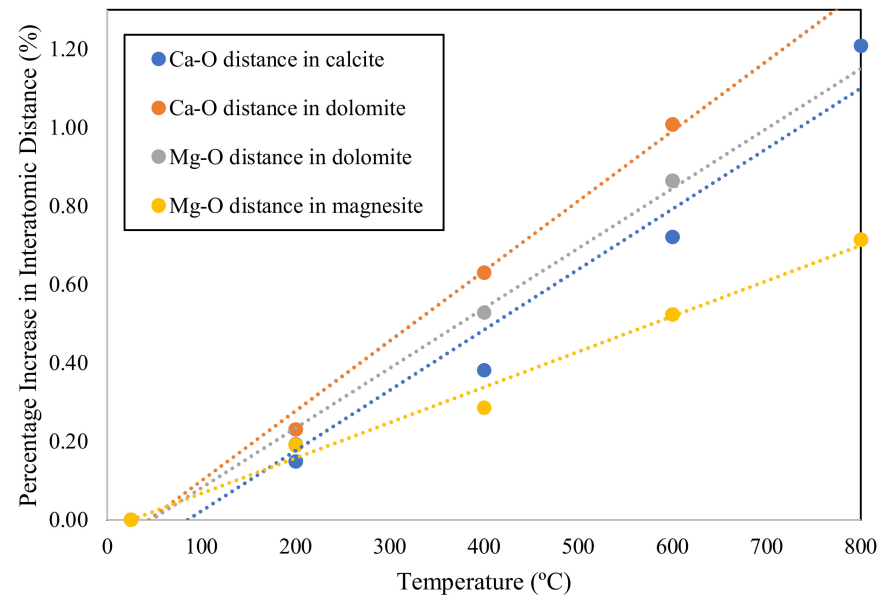


Figure 1. Percentage increase of thermal elongation in the bond length of Ca-O and Mg-O adapted from Reeder and Markgraf [52].

As concerns the thermal dislocation of the carbonate group in dolomite, it is intermediate between the calcite and magnesite. In calcite, the displacement of the carbonate group is the result of rotational disorder, which is the rotary oscillation about the three-fold axis [55]. In the case of dolomite and magnesite, the influence of the Mg-O bond confines the motion of the oxygen atoms. Therefore, the dislocation of the carbonate group in both dolomite and magnesite is less relative to that in calcite [56]. However, in magnesite, it is further less just because of the slight tilting of the basal plane. The displacement of the carbonate group contributes a minimum in the thermal deterioration of carbonate rocks. Previous studies show that, in calcite, the change in orientation of the carbonate group even at elevated temperature (i.e., 600 °C) is $<0.5^\circ$ as compared to its ambient conditions [49]. In dolomite, the adjacent layers share corners with different octahedra. In other words, the carbonate group makes the bond with unlike cations that further restrict its motion. This signifies that rotation of the carbonate group is not a decisive factor in the thermal deterioration of carbonate rocks. The thermal expansion of calcium and magnesium octahedral systems considerably affects the thermal damage of the carbonate rocks.

2.3. Thermal Cracking and Microstructural Variations

Carbonate rocks exposed to a temperature window of 500 °C to 1500 °C considerably experience an alteration in their mineral composition, mineral strength, physical structures, textural characteristics, and grain cementations [57]. Under the thermal environment, chemical processes, such as hydration or dehydration, red-ox reactions, deionization, mineral phase transformation, dissolution, and disappearance of bonding agents, alter the behavior of rocks to a great extent [58]. Rock–water interaction in geothermal systems, especially along the fault zones, recrystallizes the minerals through geochemical processes [59]. Each rock-forming mineral has a specific value of the coefficient of thermal expansion. Mineral elongation under thermal stresses increases the particle contact surface area and

causes microstructural changes in the rock matrix that adversely affect the mechanical, physical, and dynamic properties of rocks [60]. The phenomenon of thermal damage to rocks can be ascertained by observing the microscopic changes in rocks, such as mineral expansion under thermal stresses, grain boundary conditions, the density of intergranular and intragranular cracks, amount of the induced thermal strain, and mineral resistance to destruction [61].

Temperature levels and time of exposure are both factors that play an important role in the thermal degradation of different rocks. For example, in the case of crystalline rocks at a low temperature, no significant changes are observed in their internal structure because of their resistant mineral composition. At a moderate level of temperature (300–500 °C), minerals start to expand and make closures at grain boundaries that lead to a reduction in the void spaces. At a high level of temperature (>500 °C), thermal stresses in the rocks exceed the threshold limit of minerals' coefficient of thermal expansion, which causes mineral damage and relaxation at their contact boundaries. Researchers observed that mineral expansion in crystalline rocks occurs at a temperature ranging from 400 °C to 600 °C, and, beyond this temperature, rocks start to deform plastically [62,63]. On the other hand, in the case of carbonate rocks, at a low level of heating (<300 °C), the relaxation phenomenon starts at the grain contact boundaries because their minerals and bonding agents are less resistant to thermal damage. On heating limestones at temperatures > 600 °C, the emission of carbon dioxide with the decomposition of calcium carbonates weakens the limestone [57].

Advanced techniques such as X-ray diffraction (XRD), X-ray fluorescence (XRF), computerized tomography scanning (CT), and scanning electron microscopy (SEM) have been used widely in high-temperature rock mechanics to investigate microscopic variations in rocks that give an idea to understand macroscopic changes [64–67]. Furthermore, a summary of the major findings regarding the microscopic variations in thermally damaged carbonate rocks is described in Table 2.

Table 2. Summary of major findings regarding the microscopic evaluation of the thermally damaged carbonate rocks.

Temperature Range	Major Findings	Reference
200–800 °C	They analyzed the thermally treated limestones using scanning electron microscopy. They showed orientation of thermal tension and shear cracks developed in limestone. The cracks were straight, curved, parallel, vertical, oblique, and crossed layers.	[64]
100–500 °C	They studied the monomineralic carbonate rocks subjected to various temperature ranges. They observed that, in these kinds of carbonate rocks, thermal damage was the function of anisotropic dilation of calcite and shrinkage of clay minerals. The mineral expansion was observed at a temperature range of 100–200 °C, whereas intergranular and intragranular cracking was noted at 300–500 °C.	[13]
25–600 °C	They demonstrated the thermal deterioration of the limestone in terms of spectral reflectance. They found that, at an initial level of temperature, mineral expansion under elastic constraints increased the spectral reflectance, and, at a temperature above 500 °C, the thermal degradation of minerals decreased their spectral reflectance.	[20]
20–1000 °C	He investigated the effect of mineral crystal structures on the thermal behavior of carbonate rocks. In the case of dolostone, he observed that larger crystals of dolomite minerals decomposed more than the dolostone containing the smaller size dolomite crystals.	[65]
25–800 °C.	XRF technique was used to investigate the microstructural changes in limestones. They noticed an appreciable alteration in the percentage of the mineral content at a temperature window of 400–700 °C.	[66]
20–800 °C	They studied microstructural variations in carbonate rocks and found no noticeable changes in the chemical composition at a temperature below 400 °C. Furthermore, they observed that calcite and dolostone were decomposed at 400–500 °C and clay minerals started to decay at a temperature above 500 °C. In the case of trace minerals and impurities, their concentration was decreased gradually up to 400 °C and then increased sharply above 600 °C.	[67]

3. Crack Initiation and Propagation

Griffith's theory provides a solid base to ascertain the concept of fracture initiation in brittle materials. His work mainly focuses on the initiation of the tensile failure at the tip of the elliptical cracks. He studied the fracture initiation in glass material under biaxial loading. Later on, researchers applied this concept to the rocks subjected to the triaxial loading conditions [68]. This extended work undergoes the analysis of stresses around the minute defects or cracks under a three-dimensional state of stress i.e., σ_1 , σ_2 , and σ_3 . It is noted that, at the tip of the crack, the confining stress, σ_2 , does not contribute significantly to tensile failure initiation (see Figure 2). Therefore, it is analogous to an extension of Griffith's work. Griffith's original theory deals with the crack initiation and does not consider the crack propagation or shear failure. However, in some cases, tensile failure can propagate parallel to σ_1 when tensile stress overcomes the tensile strength [69].

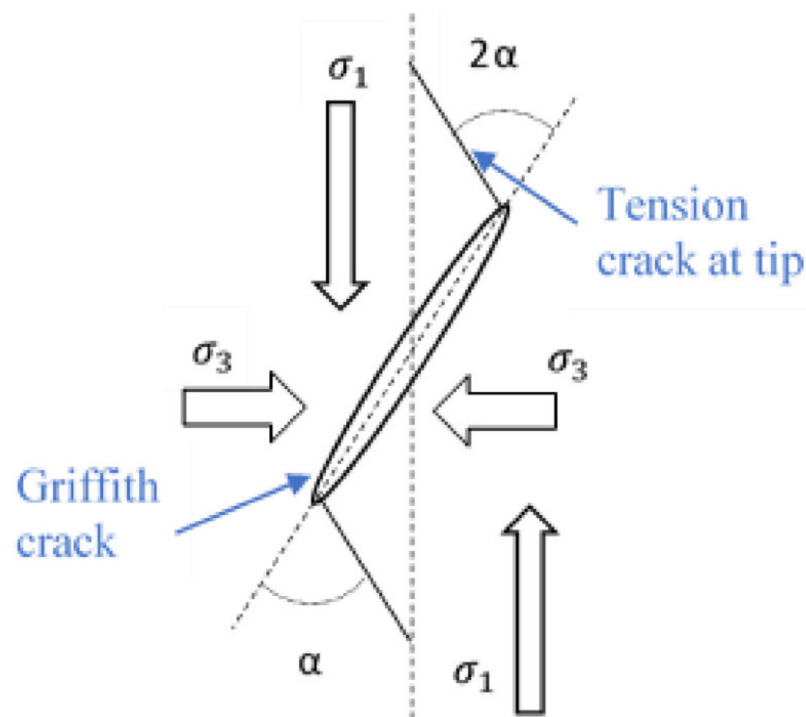


Figure 2. Crack propagation from a typical Griffith's crack in a 2-dimensional stress field adapted from Hoek and Martin [69].

In carbonate rocks, weak zones are considered along the pre-existing cracks, clay lenses, fossils, solution cavities, etc. The brittle–ductile behavior of limestone shows that strength has a negative relationship with textural characteristics [70]. Recrystallization in carbonate rocks under high temperatures significantly affects their stiffness. This process produces the void spaces in carbonates that may start a crack initiation event. Previous studies showed that, in limestone, a crack can easily propagate along the weak zones, such as bedding planes, rather than orthogonal to it [71,72]. A crack can propagate in a straight path with less energy through a medium having almost the same mechanical characteristics. However, it can bend along the grain boundaries, internal defects, clay lenses, and fossil–matrix interfaces (see Figure 3). During loading, shear failure can be noted along such bends or offsets. Apart from the above discussion, loading direction and strain rate are two important parameters that decisively play a significant role in governing crack propagation. A loading direction parallel to crack propagation helps it to propagate along grain boundaries.

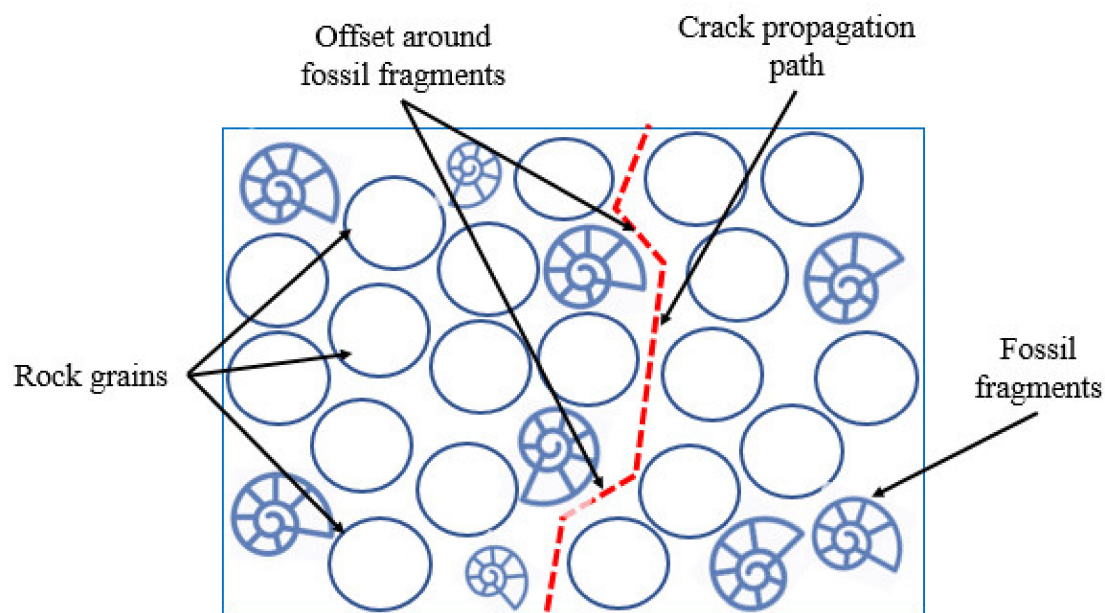


Figure 3. Schematic diagram showing crack propagation and its offset around the fossil fragments adapted from Hoagland et al. [71].

Brittle–Ductile Transition

Rocks show brittle behavior at ambient conditions, whereas high pressure and temperature shift their behavior from brittle to ductile. During brittle flow, two phenomena are very common (1) slippage and (2) twinning. When stress exceeds the critical limit, atoms in the crystal lattice slip on one another. In the case of twinning, some portion of the crystal lattice takes up an orientation that is a mirror image of the untwined parent crystal [73–75]. The stress–strain trend shows that brittle failure of rock exhibits high peak strength at a lower value of axial strain and, after failure stress, immediately reduces to a minimum level.

On the other hand, the ductile failure of a rock shows comparatively lower peak strength at a larger value of the axial strain, and, after failure, stress does not drop sharply [76]. In a loaded carbonate rock, the induced time-dependent strain initiates a microcracking event that governs the failure mechanism. The variations in the deformation behavior of limestone and dolostone under varying temperature conditions depend on the loading rate, strain amplitude, mineral composition, and internal defects [77]. Increasing axial stress induces tensile strain, which develops intergranular cracks. These cracks propagate in the direction or at an angle to the deviatoric stress. When crack propagation length becomes equal to the grain size, the coalescence of cracks enhances the stress effect; thus, the rock becomes deteriorated [78]. Therefore, researchers elucidate the rock damage mechanism in terms of micro-fissuring.

Zhao and Cao [79] explained the deformation behavior of limestone in five typical stages (see Figure 4). The stress–strain curves at ambient temperature and low confining pressures describe the deformation response as follows: stage 1 shows a concave upward gentle slope due to the nonlinear closure of the preexisting cracks. The fragmental length is based on the number of cracks in the rock. Stage 2 exhibits the elastic deformation after the compaction phase. It leads the integrated stress path to a yielding point by considering rock as a continuous medium. Stage 3 illustrates a concave downward slope leading to a threshold point. In this phase, stable microcracks develop and propagate in the direction or at an angle to the deviatoric stress. Preexisting cracks, weak planes, internal defects, and damaged grain boundaries contribute to this phase. Stage 4 depicts the concave downward curve leading to a peak strength point. It deals with the rock internal damage phase where

unsteady growth and coalescence of microcracks are prominent. Stage 5 demonstrates the post-failure curve after peak strength.

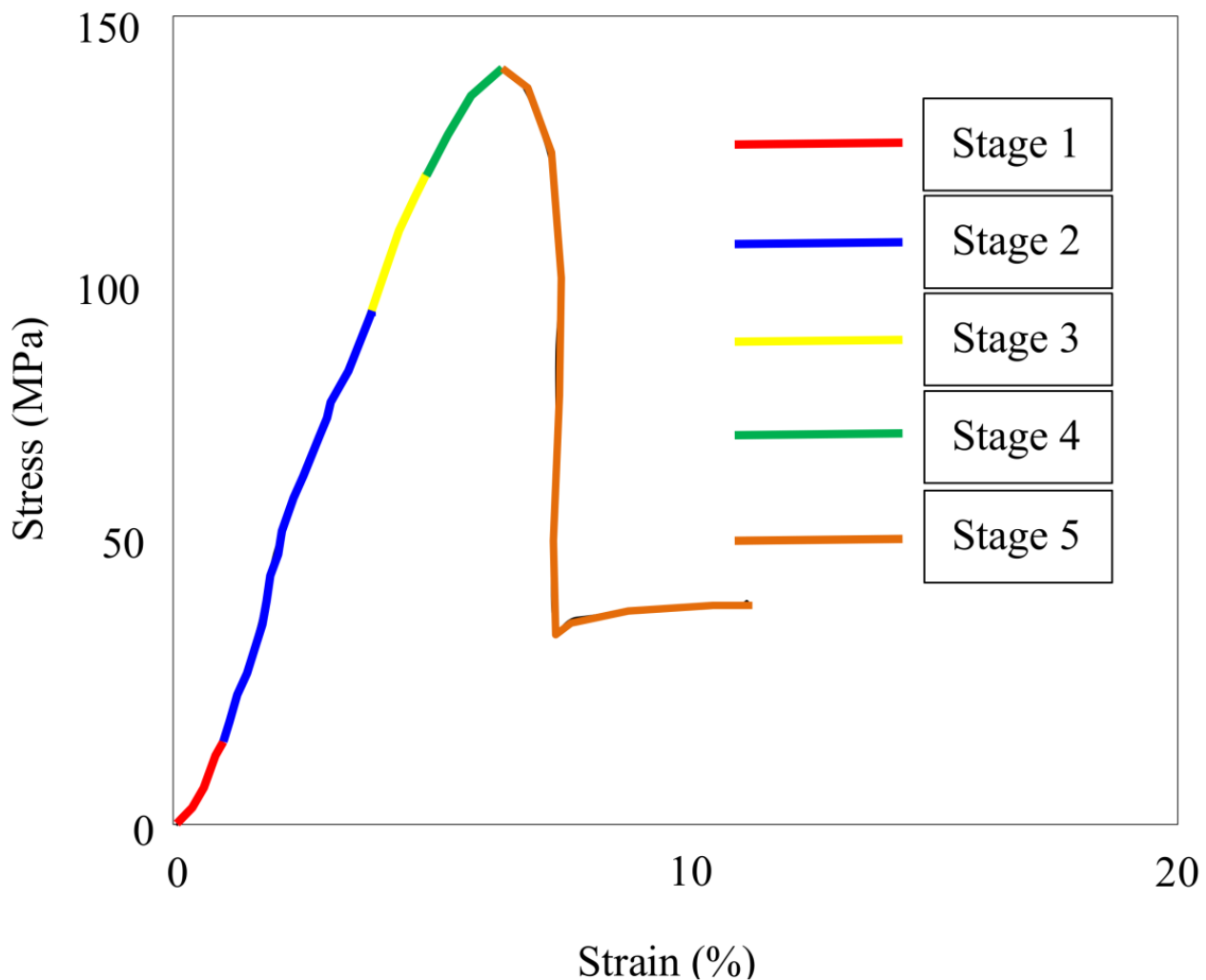


Figure 4. The behavior of limestone under compression test at ambient temperature and low confining pressure adapted from Zhao and Cao [79].

Mao et al. [80] performed a series of uniaxial compression tests on limestones heated at various temperature ranges (25–800 °C). As shown in Figure 5, at a temperature window of 25 to 600 °C, pre-failure stress–strain curves show a very similar kind of trend in their dilation phase, linear-elastic deformation phase, and brittle deformation phase. A nonlinear increment is found in their peak strength, with the rise in temperature up to 600 °C. Above a temperature of 600 °C, stress–strain curves give a lower value of peak strength at a comparatively larger value of axial strain, which is a clear indication of plastic deformation. In another study, Castagna et al. [81] performed a triaxial compression test on thermally treated limestones (20–600 °C) at room temperature and low confining pressure of 15 MPa. The thermally treated samples showed almost the same peak stress before 450 °C, and, beyond this temperature, abnormal behavior was noted, as shown in the stress–strain curves (see Figure 6). With the increase in temperature, the percentage of strain accumulation also increases, and, at 600 °C, a limestone sample can endure maximum strain at the cost of minimum peak stress. This anisotropic strain-softening behavior signifies the transition of phase from brittle to ductile. It is evident from both uniaxial and triaxial testing that carbonate rocks show ductile behavior above the critical temperature of 400 to 500 °C.

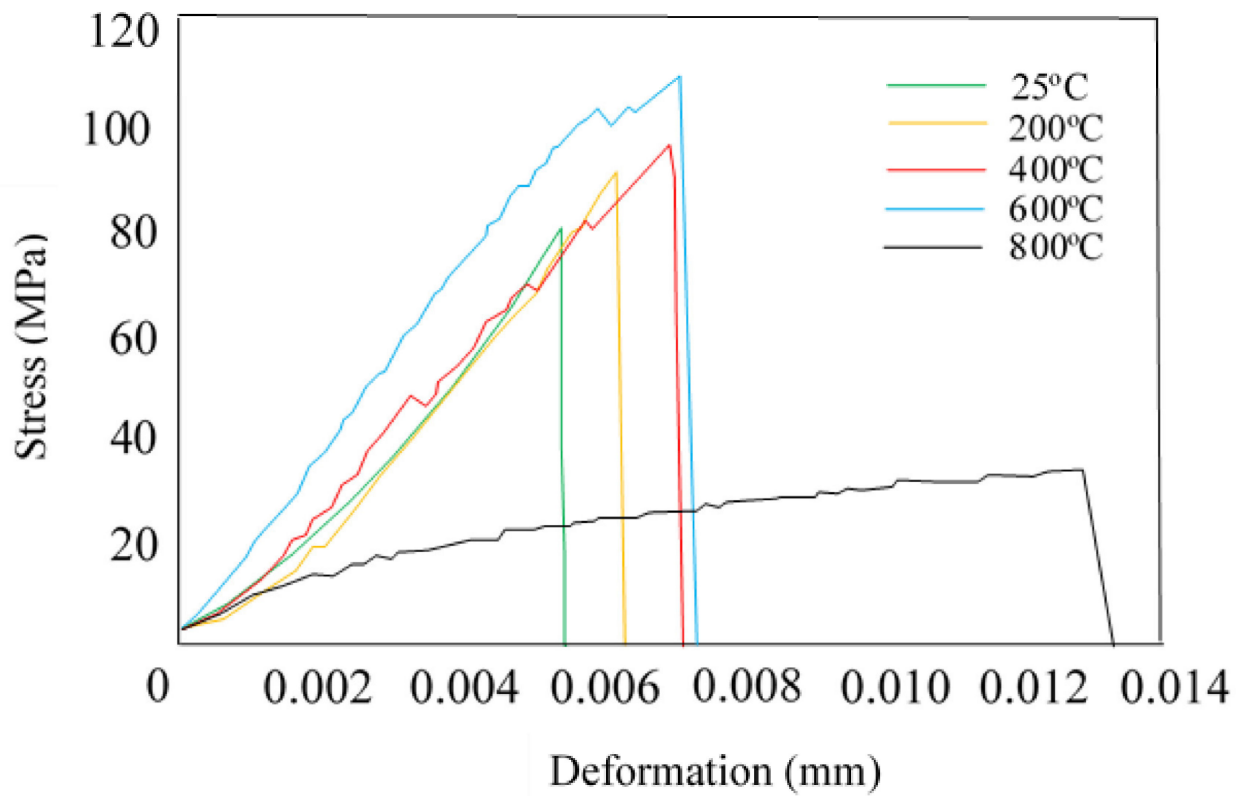


Figure 5. Uniaxial compression test on limestone subjected to various temperatures adapted from Mao et al. [80].

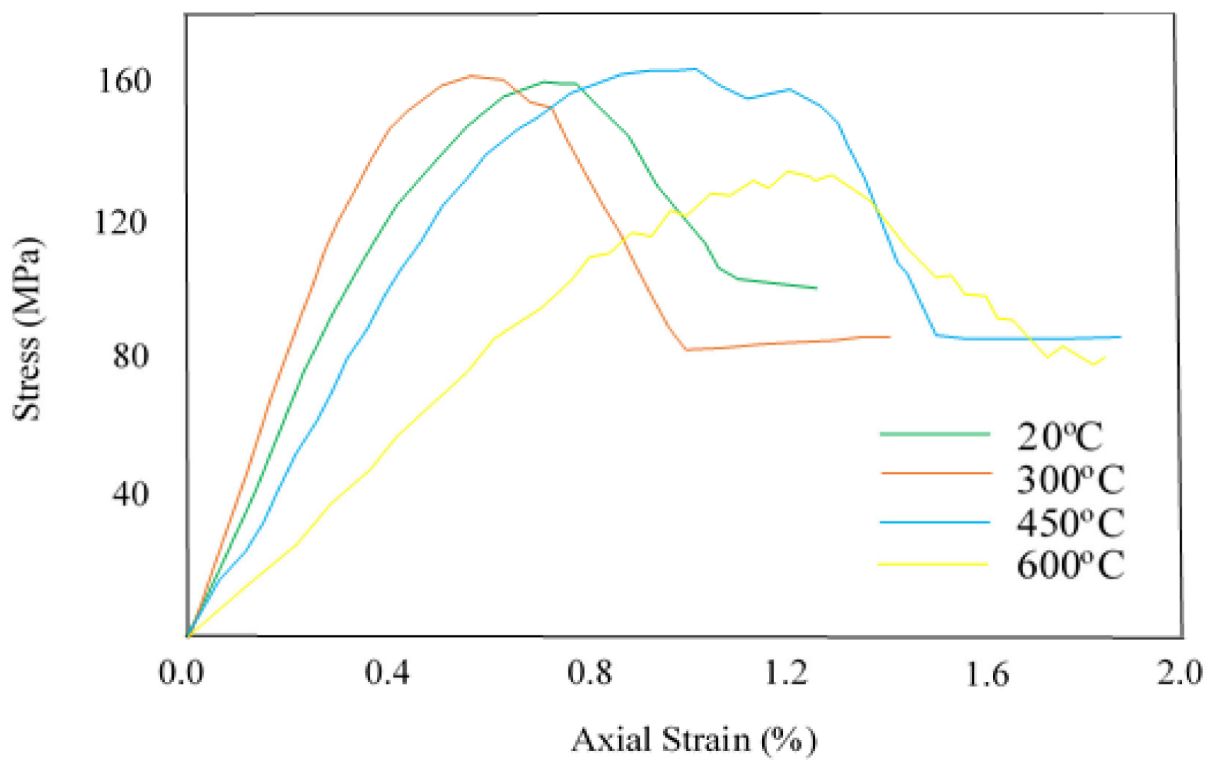


Figure 6. Triaxial compression on limestones subjected to various temperatures adapted from Castagna et al. [81].

Brittle–ductile transformation under a thermal environment considerably depreciates the mechanical properties of rocks [82–84]. Table 3 briefly describes the effect of thermal deterioration on the mechanical characteristics of carbonate rocks.

Table 3. A brief description of major findings regarding the variations in mechanical properties of the thermally damaged carbonate rocks.

Material Properties	Major Findings	Reference
Compressive Strength	At a temperature of 100–500 °C, linear changes were observed because ultimate rock strength was higher than the induced thermal strains. Above 500 °C, about 70% reduction was recorded in the peak strength, which was a result of plastic deformation.	[82]
Compressive Strength & Elastic Modulus	They tested the San Julian’s calcarenite at a temperature of 100–600 °C to investigate the behavior of porous carbonate rocks. At 600 °C, they found a reduction in peak strength and elastic moduli by 35% and 75%, respectively.	[83]
Compressive Strength & Elastic Modulus	They studied the mechanical behavior of thermally deteriorated carbonate rocks at a temperature window of 25–900 °C. They observed that, beyond the brittle–ductile transformation phase, the slippage–twining effect in crystal lattice governed the plastic deformation and significantly reduced the peak strength and elastic modulus	[84]
Compressive Strength & Elastic Modulus	They found a significant reduction in elastic modulus at a temperature of 600 °C. Beyond this critical temperature (i.e., 600 °C), rock strength dropped to 81%. The decomposition of carbonate at elevated temperature was considered the main reason for depreciation in mechanical characteristics.	[9]
Compressive & Tensile Strength	They investigated the thermal cycling effect on carbonate rocks at a temperature of 200 °C. They noticed a considerable decrement in compressive strength and tensile strength of dolostone by 27% and 25%, respectively.	[6]

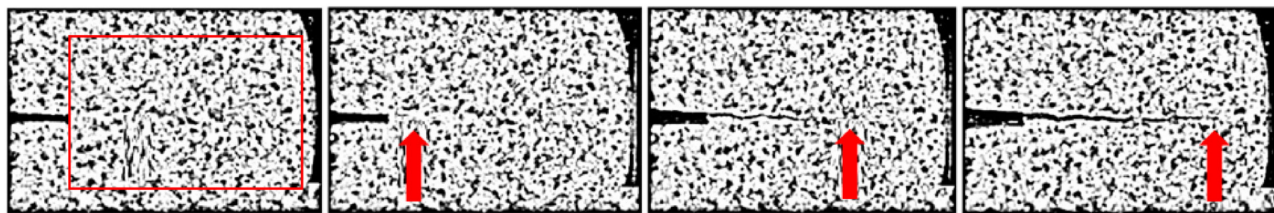
4. Dynamic Fracture Toughness and Failure Modes

Rocks show a more sensitive response against dynamic loading than static loading [85]. The behavior of rocks or rock mass under dynamic loading is considered different as compared to their behavior when subjected to static loading conditions. The high rate of dynamic loading significantly affects the microstructural behavior of rocks [86]. Dynamic loading of rock material can be referred to as destructive (dynamic compression test, dynamic tension test, impact test, etc.) or nondestructive (transmission and attenuation of stress waves). In the case of perfectly elastic conditions, materials regain their original position after the removal of stress. However, rock is not a perfectly elastic material, which is why induced strains are not 100% recoverable even in the elastic domain [87]. Rocks experience a considerable alteration in their behavior when exposed to cyclic thermal loading for a longer period. For example, a report published in the year 2000 revealed that heatwaves through radioactive waste repositories may take 50 years to induce thermal stresses of about 40 to 50 MPa in country rocks [88]. This implies that the integration of microscopic deformations over time leads to macroscopic changes.

Researchers have studied the dynamic behavior of different rocks under destructive and nondestructive dynamic loadings [8,89–99]. They found that an increasing loading rate appreciably affects the dynamic response of rocks. At a high strain loading rate, rock fracture toughness, internal defects, and other microstructural characteristics exhibit different trends than their microscopic variations observed under quasi-static loading conditions. The dynamic stiffness of different rocks has been reported to be four to eight times higher than their static stiffness [100]. Several studies have been conducted to ascertain the dynamic response of rocks at their ambient conditions, but there is limited literature available that evaluates the dynamic behavior of thermally deteriorated rocks or rock mass [101]. High-temperature rock dynamics is an important subclass of rock mechanics, and it requires extensive experimental study. The ISRM has suggested using the Split Hopkinson Pressure Bar (SHPB) testing apparatus to evaluate the dynamic behavior of rocks. Still, some problems need to be addressed to ameliorate acquired testing results.

These issues are as follows: rate-dependent constitutive modeling, validation of numerical simulations, high-rate deformation measurements, etc. [86].

Under dynamic loading, microstructural variations in rocks are referred to as fracture properties, including fracture initiation, fracture propagation, fracture velocity, and energy absorption [96–98]. Zhang [86] performed a dynamic notched semi-circular bending (NSCB) test on carbonate rock at room temperature to study the fracture initiation toughness. Figure 7 shows a frame of four pictures captured by the high-speed camera at different stages of the test. The first frame at 0 μ s shows a zone of interest, the second frame displays the crack initiation phenomenon at 40 μ s, and the next frames demonstrate the crack propagation phenomenon up to the last frame, where the crack is visible at 64 μ s.



Zone of Interest at 0 μ s Crack Initiation at 40 μ s Crack Propagation at 56 μ s & 64 μ s

Figure 7. High-speed camera images show crack initiation and propagation under dynamic loading adapted from Zhang [86].

To ascertain the dynamic behavior of thermally treated carbonate rocks, Ping et al. [89] tested the limestone samples at the temperature window of 25 to 600 °C using the SHPB at an impact pressure range of 0.4 to 0.9 Mpa. Figure 8 shows that the dynamic stress–strain curves exhibited three stages, which include elastic phase, yielding phase, and failure point. At a constant temperature, the slope of the linear relationship between dynamic stress–strain increased with the increase in impact pressure. However, the increasing temperature gradually depreciated the elastic phase and enhanced the yielding phase up to the failure point under brittle–ductile transformation in which rock can withstand greater strain at minimum stress. The same results were also reported by Yu et al. [91] while testing thermally treated limestones (25–900 °C) under quasi-vacuum and air-filled environments. The failure modes of limestone subjected to dynamic compression were observed as chip-shaped fragmentation and axial splitting with shear cracks. The increasing impact pressure with constant temperature broke the limestone into smaller fragments due to the application of high incident energies. Similarly, increasing temperature with constant impact pressure damaged the limestone with a greater degree of fragmentation because of its internal thermal cracking. However, the degree of failure at ambient conditions was quite low as compared to the provided elevated temperature (i.e., 600 °C).

High-frequency stress waves through rocks induce low strain. They are unable to exceed the threshold limit of static friction between the rock grain boundaries or weak planes [102]. The attenuation of these waves provides valuable information about rock internal defects or damage. Researchers have been using ultrasonic wave velocities to ensure thermal damage in rocks after their heat treatment at various ranges of temperature. Table 4 describes the major findings of past researchers regarding how thermally treated carbonate rocks behave under destructive and nondestructive dynamic loading.

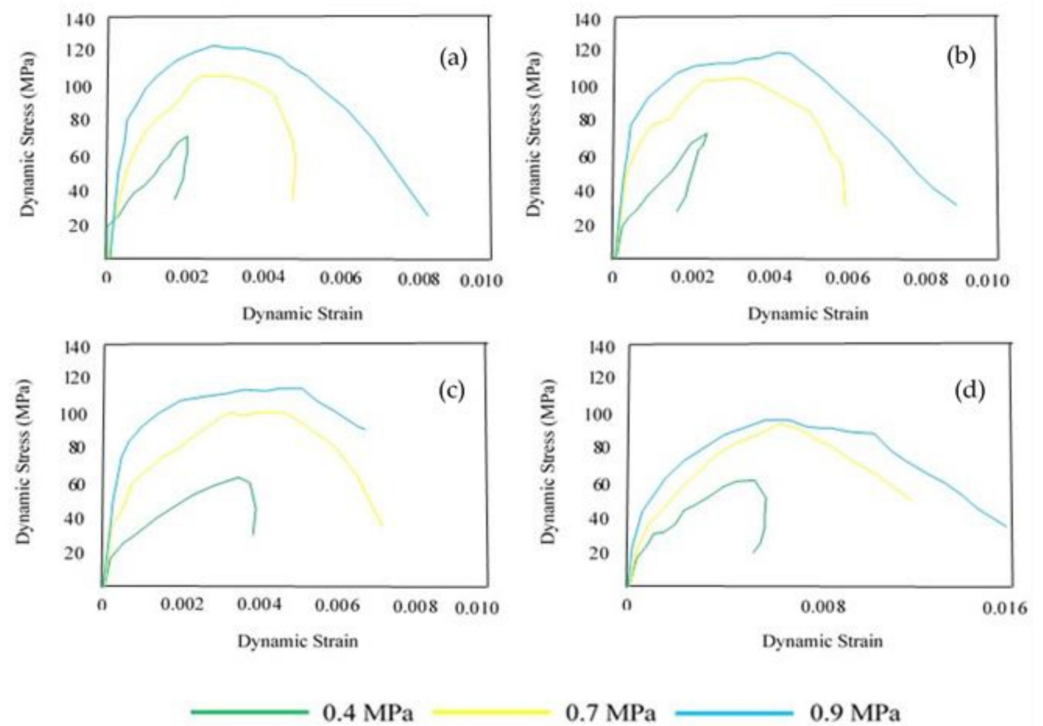


Figure 8. Limestone specimens heated at (a) 25 °C, (b) 200 °C, (c) 400 °C, and (d) 600 °C show their stress–strain curves under dynamic loading conditions adapted from Ping et al. [89].

Table 4. A brief description of major findings regarding the variations in dynamic properties of the thermally damaged carbonate rocks.

Material Properties	Major Findings	Reference
Dynamic Compressive Strength	They studied the thermal effect on the dynamic behavior of carbonate rock in two different scenarios. Firstly, they tested the heated rock specimens at a temperature above 300 °C. Secondly, they tested the air-cooled thermally treated rock samples. They found very similar results in both cases and concluded that, at this temperature range, thermal deterioration did not affect the dynamic strength of rocks to a great extent.	[82]
Dynamic Elastic Modulus	They noticed a linear change in the dynamic elastic modulus of porous carbonate rocks with rising temperatures. They recorded decrements in limestones by 10%, 60%, and 75% at 200 °C, 400 °C, and 600 °C, respectively.	[83]
Dynamic Compressive Strength	They performed a uniaxial impact compressive load test on limestone samples to discern their dynamic–mechanical behavior. The test results showed that the dynamic compressive strength of limestone had an exponential rise with the strain rate under an increasing impact pressure.	[93]
Dynamic Compressive Strength & Dynamic Elastic Modulus	He investigated the effect of temperature on the dynamic properties of carbonate rocks. He tested limestone at undamaged, moderate damaged (heated at 450 °C), and high damaged (heated at 800 °C) conditions under an increasing strain rate. He noted that, on account of anisotropic effects, the dynamic strength of damaged samples was found greater than the strength of undamaged samples. Furthermore, he found that the elastic modulus calculated by using ultrasonic wave velocities was dropped to 92% at 800 °C.	[92]
Dynamic Elastic Modulus	They heated the limestone from its ambient temperature to 900 °C and found a 70% reduction in dynamic elastic modulus at 600 °C. This temperature was considered as a critical temperature after which limestone started to change its behavior from brittle to ductile.	[91]
Damping Ratio, Damping Capacity, & Loss Factor	They studied the cyclic effect of temperature on the dynamic properties of selected carbonate rocks. In the case of dolostone, they noticed a significant appreciation in its damping ratio, specific damping capacity, and loss factor by 15%, 13%, and 12%, respectively.	[90]
Dynamic Elastic Modulus	They observed that the thermal cycling effect significantly reduced the dynamic elastic modulus of dolostone by 38% at 200 °C.	[8]

5. Thermal Deterioration of Porous Network

The physical properties of rocks greatly help to anticipate the behavior of carbonate rocks under different loading conditions. The anisotropic character of such rocks is attributed to their depositional environment, diagenesis conditions, past stress histories, pressure, temperature, and chemistry of pore fluids. The heterogeneity in the physical characteristics depends on the rock fabric and microstructures [103]. The microstructural patterns are generally defined by the texture (size, shape, and sorting), density, cementation between the particles, the orientation of particles, and cracks under regional or local stresses [104]. These microstructural variations immensely affect the porous network and transport properties of carbonate rocks. The porosity, permeability, and acoustic waves attenuation are the most widely studied physical parameters to evaluate the physical–mechanical behavior of carbonate rocks and other materials under undamaged or damaged conditions [7,12,13,87,104–111].

The porosity of the limestone and dolostone mainly consists of two-pore systems: primary pores and secondary pores. The natural fractures or breaks, cavities, organic growth, and dissolution of material in the cracks due to fluid transportation are the main factors that enhance the porosity to a large extent [104]. The size of the intergranular and intragranular pores falls within the range of 30 to 50 μm , whereas secondary pores include micro-fissuring, vugs, the disappearance of cementation, and the opening of grain boundaries are typically in the range of 0.5 to 50 mm [112]. The aforementioned pore sizes were measured at ambient conditions. These opening sizes can be considerably larger than their documented values when rocks are subjected to high temperatures. The transport properties of carbonate rocks depend on pore geometry, connectivity, and tortuosity. The permeability is an important physical parameter that provides valuable information about the connectivity of primary or secondary pores. The high porosity of a rock is not referred to as its high permeability; rather, it is characterized by the connectivity of the pores [113]. Like porosity and acoustic waves, permeability is also sensitive to temperature. Several studies have been conducted to investigate the thermal weakening effect on the permeability of carbonate rocks. Table 5 describes the major development in the evaluation of transport properties of thermally exploited carbonate rocks.

Acoustic wave transmission through limestone is mainly governed by grain contact and cementation. The strong bond or cementation between rock grains makes it stiff, which favors wave propagation. The microcracks, vugs porosity, and pore aspect ratio significantly affect the acoustic wave velocities [103]. The primary minerals in limestone and dolostone have specific values of elastic bulk modulus and the coefficient of thermal expansion. The temperature beyond the threshold limit of these properties significantly alters the physical–mechanical behavior of these rocks [114]. High temperature ($>500\text{ }^{\circ}\text{C}$) enhances secondary porosity by developing micro-fissures, opening grain contact boundaries, removing cementation between grains, and accelerating chemical reactions that ultimately reduce physical characteristics and acoustic wave velocities to a minimum level [115–119].

Table 5. Summary of major findings regarding the variations in physical properties of the thermally damaged carbonate rocks.

Material Properties	Major Findings	Reference
Permeability	They noticed that, at a low temperature, crystalline limestone showed slight variations in its permeability. Moreover, the thermal cracking of limestone at a temperature above 400 °C produced an appreciable increment in its permeability.	[115]
Porosity & Permeability	They studied the temperature effect on the hydraulic and poroelastic properties of limestone. They found that the permeability of limestone was increased by 3% and 8% at the temperatures of 150 °C and 250 °C, respectively.	[116]
P-wave Velocity	They investigated the thermo-physical behavior of limestones at varying temperatures. They noticed slight variations in P-wave velocities at a temperature of 150 °C and a linearly decreasing trend by 55% at 500 °C.	[13]
P-wave Velocity	He studied thermal effects on the physical properties of carbonate rocks. At the initial temperature (i.e., 200 °C), only 4% depreciation was recorded in the P-wave velocity. However, at a temperature of 600 °C, due to the brittle–ductile transformation, its value reduced to 36%.	[12]
Porosity	They investigated the thermal damage effect on the porosity of air-cooled and water-cooled limestone specimens. They found that, at 200 °C, both limestone samples showed a very similar increase in porosity (i.e., 1–1.5%). At the temperature of 300 °C, air-cooled and water-cooled limestone samples showed a 3% and 6% rise in porosity, respectively. On further increase in temperature of 600 °C, water-cooled limestone samples demonstrated slight variations in their porosity, whereas air-cooled limestone samples followed a linear increasing trend in porosity by 11%.	[83]
Porosity	They observed no significant variations in the total porosity of carbonate rocks at ambient temperature. However, at 800 °C, ductile behavior considerably changed the porosity by 13%.	[117]
Permeability	They found a reduction in the permeability of pre-heated fractured carbonate rocks with a slight rise in temperature (i.e., 60 °C). The obvious reason for this behavior is that, at a low temperature, rock dilates to enhance stiffness, which ultimately reduces permeability. On the other hand, at higher temperatures, fluid transport properties improve on account of thermal cracking and brittle–ductile transformation.	[118]
Porosity	They evaluated the porosity of carbonate rocks under different conditions. For porous dolostone, they found that the temperature effect was larger than the pressure effect and the rate of dissolution was inversely proportional to temperature.	[119]
Permeability	They observed no changes in the permeability of limestone at low temperature and then recorded an increase in permeability by 2%, 10%, and 126% at the temperatures of 600 °C, 700 °C, and 800 °C, respectively. Beyond the temperature of 700 °C, limestone lost its integrity, which is why a sharp increase was noted in its permeability.	[106]
P-wave Velocity	They observed that thermal exploitation reduces the stiffness of porous rocks, turns them into a more compressible state, and hinders wave propagation by limiting their quality.	[90]
P-wave Velocity	They studied the coupling effect of high temperature and liquid nitrogen quenching on the physical characteristics of limestones. They found an appreciable reduction in P-wave velocities by 47% and 88% at a temperature of 400 °C and 600 °C, respectively.	[105]

Heat Transport Properties

Heat transport properties of carbonate rocks have great importance in many engineering applications. These thermal properties provide a good set of information to discern the behavior of carbonate rocks under the thermal environment. The thermal response of

materials subjected to thermal stresses can be ascertained in terms of their thermal conductivity (k), thermal diffusivity (D), coefficient of thermal expansion, heat transfer capacity (C_p), and thermal damage factor [120]. The variations in thermal properties of rocks at ambient temperature or beyond it have been studied by several past researchers [121–126]. However, the imperfection of the physical contact methods often underestimated or overestimated the thermal properties of various rocks and minerals. For example, Clark [127] studied the effect of temperature on the coefficient of thermal expansion of granite and limestone at a temperature range of 20 to 100 °C. He found that both rocks were expanded at almost the same rate. Later on, limestone's dilation was observed much lower than the granite [128]. The application of non-physical contact methods, such as laser flash analysis (LFA), in measuring the thermal transport properties of rocks has been reported by many researchers [10,129–132]. They highlighted some problems of using the conventional approaches and found that laser flash analysis has a competitive edge over other physical contact methods. They proposed LFA as the best technique to accurately measure the thermal properties of rocks.

Thermal diffusivity is the ratio of thermal conductivity to the product of density and heat capacity. This property is the function of temperature, and its value decreases as the temperature increases. Thermal diffusivity has a direct relationship with thermal conductivity and an inverse relationship with density and heat capacity. At a high temperature (>500 °C), due to thermal cracking and microstructural variations in rocks, thermal conductivity starts to decline, which ultimately reduces thermal diffusivity. Conversely, in the case of density and heat capacity, the increasing temperature slightly affects the density at the macroscopic level as a result of the low dilation of minerals [133]. Therefore, small variations in density do not significantly affect thermal diffusivity. Because of intercrystalline and intergranular thermal cracking, the rock begins to absorb more thermal energy, which is why heat capacity increases and thermal diffusivity depreciates with the temperature. When an intact and continuous rock specimen is heated, the initiated thermal cracking event improves its porosity and, thus, the material shows a slightly larger volume than that of an uncracked state. On reheating a thermally cracked rock specimen, expected dilation does not happen and the material becomes comparatively stiffer because of mineral expansion in the cracked spaces [124].

Unlike fluid transport properties for which connected pores are required, the thermal conductivity of limestone is mainly governed by the mineral composition, porosity, and grain contact surface area. High temperature deteriorates rock fabric, which leads to a reduction in thermal conductivity and thermal diffusivity. Merriman et al. [10] discussed the temperature-dependent thermal transport properties of carbonate rocks. At a temperature range of 27 to 327 °C, calcite-rich limestone showed lower thermal diffusivity than the thermal diffusivity of its primary mineral (calcite). Furthermore, they found that thermal conductivity dropped to 50% at 327 °C. Shen et al. [134] studied the thermophysical characteristics of limestones and sandstones at a temperature of −30 to 1000 °C. In the case of limestone, they observed that, at stage 1 (−30–20 °C), the thermal properties were slightly improved by 8% due to freezing of pore fluids, at stage 2 (20–600 °C), an increasing temperature up to the 600 °C induced thermal tension cracks within the rock matrix that linearly reduced the thermal properties, and, at stage 3 (600–1000 °C), the ductile behavior of the rock sharply decreased the thermal properties. Miao and Zhou [135] investigated the temperature dependence on thermal transport properties of carbonate rocks at a temperature range of 25 to 700 °C. They noticed a linear decrement in thermal conductivity and thermal diffusivity by 61% and 78%, respectively, from ambient temperature to critical temperature. Khan et al. [136] recorded a similar depreciation trend in the thermal properties of carbonate rocks, as reported in previous studies. They found a reduction of 36% in thermal conductivity and a decrement of 52% in the thermal diffusivity of post-heated samples tested at the low-temperature range of 20 to 170 °C. Increasing temperature reduces the thermal transport properties of rocks, whereas increasing pressure enhances the thermophysical properties of rocks. The coupling effect of temperature and

pressure at a very high level starts to counter each other and does not follow the linear trend [137–139]. The variations in the thermal transport properties of heated carbonates reported by past researchers have been displayed in Figure 9.

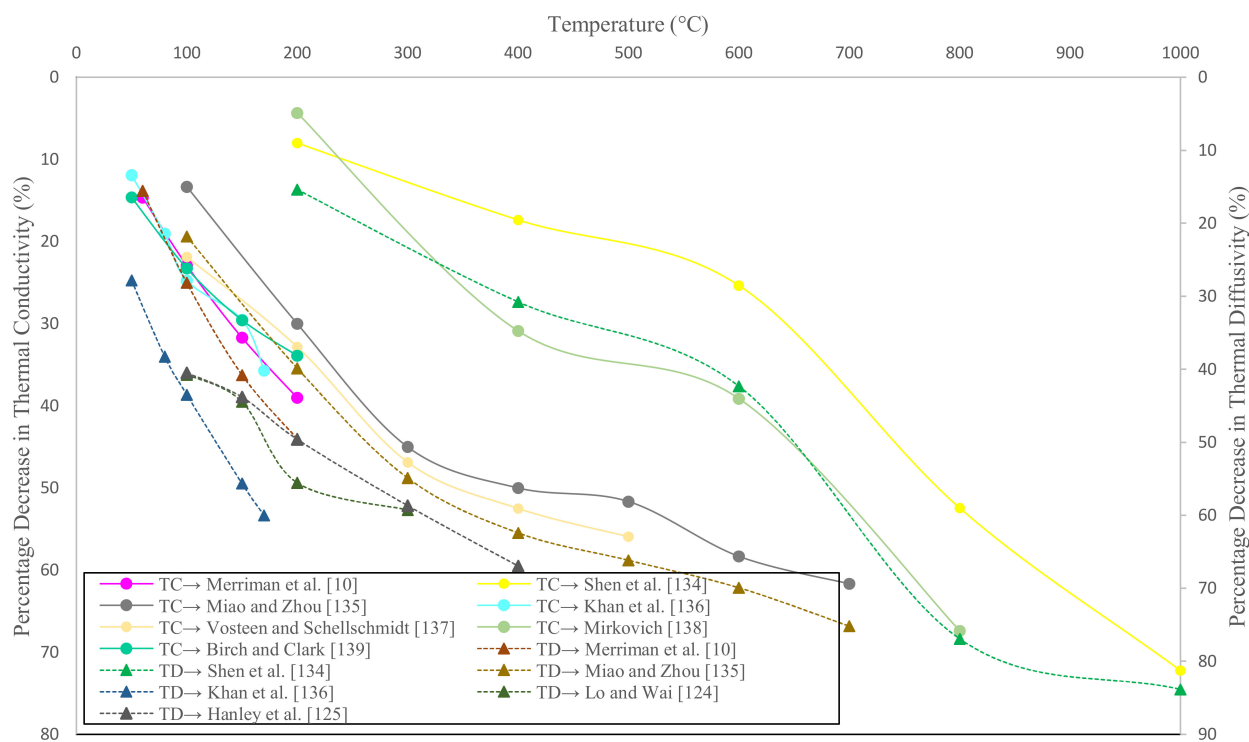


Figure 9. Effect of temperature on thermal conductivity and thermal diffusivity of carbonate rocks tested at various temperatures. TC and TD represent the thermal conductivity and thermal diffusivity, respectively.

6. Conclusions

This paper investigates the effect of thermal damage on the behavior of carbonate rocks in terms of their mineralogical, mechanical, dynamic, physical, and thermal properties. It covers the literature review of more than 50 years of research work to highlight the advancements in high-temperature rock mechanics to ascertain the behavior of carbonate rocks under the thermal environment. The full understanding of the engineering characteristics of rocks under varying temperature and loading conditions depends upon the theoretical framework, experimental approaches, reliable instrumentation, constitutive modeling, and numerical simulations.

Temperature significantly affects the mineralogical properties of porous rocks. It alters their mineral composition, mineral strength, physical structures, textural characteristics, and bonding agents by initiating some processes, such as hydration or dehydration, red-ox reactions, deionization, mineral phase transformation, melting, microcracking, and deterioration of bonding agents. Unlike crystalline rocks, carbonate rocks degrade at comparatively low temperatures. At a temperature window of 400 to 500 °C, their primary and secondary minerals decompose, whereas clay minerals and other materials start to decay beyond the critical temperature. A high temperature (>600 °C) breaks the calcium carbonate, calcium bicarbonate, and magnesium carbonate; thus, emission of carbon dioxide weakens the limestone and dolostone.

Under static loading conditions, the stress–strain curves of thermally deteriorated limestone describe its deformation behavior in five stages, including (1) compaction phase, (2) elastic deformation phase, (3) microcracking phase, (4) peak strength phase, and (5) post-failure phase. An increasing temperature considerably decreases the peak compressive strength and static elastic modulus. Carbonate rocks show brittle behavior above a tem-

perature of 400 °C. The brittle–ductile transformation phase begins at a temperature range of 400 to 500 °C, and, beyond this critical temperature, their ductile behavior becomes dominant because of the slippage–twining effect in the crystal lattice.

High-temperature rock dynamics provides a solid base to discern the dynamic behavior of carbonate rocks subjected to varying temperatures. The variations in their dynamic properties at the macroscopic level are referred to as their fracture characteristics, including fracture initiation, fracture propagation, fracture density, fracture velocity, and energy absorption. Recent and past studies show that an increasing impact pressure and strain rate ameliorate dynamic compressive strength and elastic modulus; however, the development of thermal tension cracks at elevated temperatures appreciably reduces these dynamic properties.

The variations in rocks' transport properties are mainly governed by texture (size, shape, and sorting), cementation between the particles, the orientation of particles, and natural cracks under regional or local stresses. Carbonate rocks exposed to high temperatures experience an expressive alteration in their physical response on account of the reduction in grain contact surface area, disappearance of cementation, micro-fissuring, internal defects, and intercrystalline cracking. At a temperature above 500 °C, the porosity and permeability of carbonate rocks improve sharply, whereas P-wave velocities decline nonlinearly. Unlike fluid transport properties for which connectivity of pores is mandatory, their thermal properties depend upon the mineral composition and grain contact surface area. Thermal transport properties (thermal conductivity and thermal diffusivity) are sensitive to temperature. At elevated temperatures (>500 °C), the relaxation at grain boundaries and intercrystalline thermal cracking are the results of minerals' expansion beyond the threshold limit of their coefficient of thermal expansion. These factors considerably depreciate the thermal transport properties of carbonate rocks.

7. Recommendations

This review comprehensively describes the experimental findings of the damage characteristics of carbonate rocks subjected to gradually increasing temperature. However, in future research work, the damage mechanism of carbonate rocks will be studied under the thermal shock effect and thermal cyclic loading. This will help to achieve deep insight and anticipate the rock behavior under different states of stress. Furthermore, this study can be recommended as a reference in material stability analysis, infrastructure development, site characterization, rock mass classification, and subsurface investigations.

Author Contributions: Conceptualization and Original Draft Preparation, U.W. and H.M.A.R.; writing—review and editing, M.F.A., A.M.R. and M.E.A.-A. All authors have read and agreed to the published version of the manuscript.

Funding: This research was partly funded by Prince Sultan University.

Institutional Review Board Statement: Not applicable.

Informed Consent Statement: Not applicable.

Acknowledgments: This research is supported by the Structures and Material (S&M) Research Lab of Prince Sultan University.

Conflicts of Interest: The authors declare that they have no potential conflict of interest regarding this research work.

References

1. Behnia, D.; Ahangari, K.; Moeinossadat, S.R. Modeling of shear wave velocity in limestone by soft computing methods. *Int. J. Min. Sci. Technol.* **2017**, *27*, 423–430. [[CrossRef](#)]
2. Lai, H.P.; Wang, S.Y.; Xie, Y.L. Experimental research on temperature field and structure performance under different lining water contents in a road tunnel fire. *Tunn. Undergr. Space Technol.* **2014**, *43*, 327–335. [[CrossRef](#)]
3. Nasser, M.H.B.; Schubnel, A.; Young, R.P. Coupled evolutions of fracture toughness and elastic wave velocities at high crack density in thermally treated Westerly granite. *Int. J. Rock Mech. Min. Sci.* **2007**, *44*, 601–616. [[CrossRef](#)]

4. Heuze, F.E. High-temperature mechanical, physical, and thermal properties of granitic rocks—A review. *Int. J. Rock Mech. Min. Sci. Geomech. Abstr.* **1983**, *20*, 3–10. [[CrossRef](#)]
5. Smith, B.M.; Reynolds, S.J.; Day, H.W.; Bodnar, R.J. Deep-seated fluid involvement in ductile-brittle deformation and mineralization, South Mountains metamorphic core complex, Arizona. *Geol. Soc. Am. Bull.* **1991**, *103*, 559–569. [[CrossRef](#)]
6. Waqas, U.; Ahmed, M.F. Prediction Modeling for the Estimation of Dynamic Elastic Young's Modulus of Thermally Treated Sedimentary Rocks Using Linear–Nonlinear Regression Analysis, Regularization, and ANFIS. *Rock Mech. Rock Eng.* **2020**, *53*, 5411–5428. [[CrossRef](#)]
7. Idris, M.A. Effects of elevated temperature on physical and mechanical properties of carbonate rocks in South-Southern Nigeria. *Min. Miner. Depos.* **2018**, *12*, 20–27. [[CrossRef](#)]
8. Waqas, U.; Ahmed, M.F.; Arshad, M. Classification of the intact carbonate and silicate rocks based on their degree of thermal cracking using discriminant analysis. *Bull. Eng. Geol. Environ.* **2020**, *79*, 2607–2619. [[CrossRef](#)]
9. Yang, J.; Fu, L.Y.; Zhang, W.; Wang, Z. Mechanical property and thermal damage factor of limestone at high temperature. *Int. J. Rock Mech. Min. Sci.* **2019**, *117*, 11–19. [[CrossRef](#)]
10. Merriman, J.D.; Hofmeister, A.M.; Roy, D.J.; Whittington, A.G. Temperature-dependent thermal transport properties of carbonate minerals and rocks. *Geosphere* **2018**, *14*, 1961–1987. [[CrossRef](#)]
11. Nicolas, A.; Fortin, J.; Regnet, J.B.; Dimanov, A.; Guéguen, Y. Brittle and semi-brittle behaviors of a carbonate rock: Influence of water and temperature. *Geophys. J. Int.* **2016**, *206*, 438–456. [[CrossRef](#)]
12. Sengun, N. Influence of Thermal Damage on the Physical and Mechanical Properties of Carbonate Rocks. *Arab. J. Geosci.* **2014**, *7*, 5543–5551. [[CrossRef](#)]
13. Yavuz, H.; Demirdag, S.; Caran, S. Thermal effect on the physical properties of carbonate rocks. *Int. J. Rock Mech. Min. Sci.* **2010**, *47*, 94–103. [[CrossRef](#)]
14. Hajpál, M. *Fire Damaged Stone Structures in Historical Monuments. Laboratory Analyses of Changes in Natural Stones by Heat Effect*; CIB Publication: Salford, UK, 2010; pp. 164–173.
15. Sury, M.; White, M.; Kirton, J.; Carr, P.; Woodbridge, R.; Mostade, M.; Chappell, R.; Hartwell, D.; Hunt, D.; Rendell, N. *Review of Environmental Issues of Underground Coal Gasification—Best Practice Guide*; Report No. COAI R273 DTi/Pub URN; U.S. Department of Energy: Oak Ridge, VA, USA, 2004; Volume 4, p. 1881.
16. Behn, M.D.; Kelemen, P.B.; Hirth, G.; Hacker, B.R.; Massonne, H.J. Diapirs as the source of the sediment signature in arc lavas. *Nat. Geosci.* **2011**, *4*, 641–646. [[CrossRef](#)]
17. Philpotts, A.R.; Ague, J.J. *Principles of Igneous and Metamorphic Petrology*; Cambridge University Press: Cambridge, UK, 2009.
18. Deegan, F.M.; Troll, V.R.; Freda, C.; Misiti, V.; Chadwick, J.P.; McLeod, C.L.; Davidson, J.P. Magma–carbonate interaction processes and associated CO₂ release at Merapi Volcano, Indonesia: Insights from experimental petrology. *J. Petrol.* **2010**, *51*, 1027–1051. [[CrossRef](#)]
19. Kılıç, Ö. The influence of high temperatures on limestone P-wave velocity and Schmidt hammer strength. *Int. J. Rock Mech. Min. Sci.* **2006**, *43*, 980–986. [[CrossRef](#)]
20. González-Gómez, W.S.; Quintana, P.; May-Pat, A.; Avilés, F.; May-Crespo, J.; Alvarado-Gil, J.J. Thermal effects on the physical properties of limestones from the Yucatan Peninsula. *Int. J. Rock Mech. Min. Sci.* **2015**, *75*, 182–189. [[CrossRef](#)]
21. Lippmann, F. *Sedimentary Carbonate Minerals*; Springer Science & Business Media: Berlin, Germany, 1973.
22. Gregg, J.M.; Bish, D.L.; Kaczmarek, S.E.; Machel, H.G. Mineralogy, nucleation and growth of dolomite in the laboratory and sedimentary environment: A review. *Sedimentology* **2015**, *62*, 1749–1769. [[CrossRef](#)]
23. Asaki, Z.; Fukunaka, Y.; Nagase, T.; Kondo, Y. Thermal decomposition of limestone in a fluidized bed. *Metall. Trans.* **1974**, *5*, 381–390. [[CrossRef](#)]
24. Sanders, J.P.; Gallagher, P.K. Kinetic analyses using simultaneous TG/DSC measurements: Part II: Decomposition of calcium carbonate having different particle sizes. *J. Therm. Anal. Calorim.* **2005**, *82*, 659–664. [[CrossRef](#)]
25. Olszak-Humienik, M.; Jablonski, M. Thermal behavior of natural dolomite. *J. Therm. Anal. Calorim.* **2015**, *119*, 2239–2248. [[CrossRef](#)]
26. Karunadasa, K.S.; Manoratne, C.H.; Pitawala, H.M.; Rajapakse, R.M. Thermal decomposition of calcium carbonate (calcite polymorph) as examined by in-situ high-temperature X-ray powder diffraction. *J. Phys. Chem. Solids* **2019**, *134*, 21–28. [[CrossRef](#)]
27. Hartman, M.; Trnka, O.; Vesely, V.; Svoboda, K. Predicting the rate of thermal decomposition of dolomite. *Chem. Eng. Sci.* **1996**, *51*, 5229–5232. [[CrossRef](#)]
28. Barcina, L.M.; Espina, A.; Suárez, M.; Garcia, J.R.; Rodriguez, J. Characterization of monumental carbonate stones by thermal analysis (TG, DTG, and DSC). *Ther. Acta* **1997**, *290*, 181–189. [[CrossRef](#)]
29. Gunasekaran, S.; Anbalagan, G. Thermal decomposition of natural dolomite. *Bull. Mater. Sci.* **2007**, *30*, 339–344. [[CrossRef](#)]
30. Kök, M.U.; Smykatz-Kloss, W. Characterization, correlation, and kinetics of dolomite samples as outlined by thermal methods. *J. Therm. Anal. Calorim.* **2008**, *91*, 565–568. [[CrossRef](#)]
31. Hossain, F.M.; Długogorski, B.Z.; Kennedy, E.M.; Belova, I.V.; Murch, G.E. First-principles study of the electronic, optical, and bonding properties in dolomite. *Comput Mater Sci.* **2011**, *50*, 1037–1042. [[CrossRef](#)]
32. Jiang, J.; Ye, J.; Zhang, G.; Gong, X.; Nie, L.; Liu, J. Polymorph and morphology control of CaCO₃ via temperature and PEG during the decomposition of Ca(HCO₃)₂. *J. Am. Ceram. Soc.* **2012**, *95*, 3735–3738. [[CrossRef](#)]

33. Samtani, M.; Dollimore, D.; Wiburn, F.W.; Alexander, K. Isolation and identification of the intermediate and final products in the thermal decomposition of dolomite in an atmosphere of carbon dioxide. *Ther. Acta* **2001**, *367*, 285–295. [[CrossRef](#)]
34. Gallagher, P.; Johnson, D.W., Jr. The effects of sample size and heating rate on the kinetics of the thermal decomposition of CaCO₃. *Thermochim. Acta* **1973**, *6*, 67–83. [[CrossRef](#)]
35. Caldwell, K.M.; Gallagher, P.K.; Johnson, D.W., Jr. Effect of thermal transport mechanisms on the thermal decomposition of CaCO₃. *Thermochim. Acta* **1977**, *18*, 15–19. [[CrossRef](#)]
36. Maciejewski, M.; Oswald, H.R. Morphological observations on the thermal decomposition of calcium carbonate. *Thermochim. Acta* **1985**, *85*, 39–42. [[CrossRef](#)]
37. Engler, P.; Santana, M.W.; Mittleman, M.L.; Balazs, D. Non-isothermal, in situ XRD analysis of dolomite decomposition. *Thermochim. Acta* **1989**, *140*, 67–76. [[CrossRef](#)]
38. Rao, T.R. Kinetic parameters for the decomposition of calcium carbonate. *Can. J. Chem. Eng.* **1993**, *71*, 481–484.
39. Wang, Y.; Thomson, W.J. The effects of steam and carbon dioxide on calcite decomposition using dynamic X-ray diffraction. *Chem. Eng. Sci.* **1995**, *50*, 1373–1382. [[CrossRef](#)]
40. Rao, T.R. Kinetics of calcium carbonate decomposition. *Chem. Eng. Technol. Ind. Chem. Plant Equip. Process Eng. Biotechnol.* **1996**, *19*, 373–377. [[CrossRef](#)]
41. Dollimore, D.; Tong, P.; Alexander, K.S. The kinetic interpretation of the decomposition of calcium carbonate by use of relationships other than the Arrhenius equation. *Thermochim. Acta* **1996**, *282*, 13–27. [[CrossRef](#)]
42. Kristóf-Makó, É.; Juhász, A.Z. The effect of mechanical treatment on the crystal structure and thermal decomposition of dolomite. *Thermochim. Acta* **1999**, *342*, 105–114. [[CrossRef](#)]
43. Dash, S.; Kamruddin, M.; Ajikumar, P.K.; Tyagi, A.K.; Raj, B. Nanocrystalline and metastable phase formation in vacuum thermal decomposition of calcium carbonate. *Thermochim. Acta* **2000**, *363*, 129–135. [[CrossRef](#)]
44. Zucchini, A.; Comodi, P.; Nazzareni, S.; Hanfland, M. The effect of cation ordering and temperature on the high-pressure behaviour of dolomite. *Phys. Chem. Miner.* **2014**, *41*, 783–793. [[CrossRef](#)]
45. Cai, J.; Wang, S.; Kuang, C. A modified random pore model for carbonation reaction of CaO-based limestone with CO₂ in different calcination-carbonation cycles. *Energy Procedia* **2017**, *105*, 1924–1931. [[CrossRef](#)]
46. Subagio; Wulandari, W.; Adinata, P.M.; Fajrin, A. Thermal decomposition of dolomite under CO₂-air atmosphere. *AIP Conf. Proc.* **2017**, *1805*, 040006.
47. Momenzadeh, L.; Moghtaderi, B.; Buzzi, O.; Liu, X.; Sloan, S.W.; Murch, G.E. The thermal conductivity decomposition of calcite calculated by molecular dynamics simulation. *Comput. Mater. Sci.* **2018**, *141*, 170–179. [[CrossRef](#)]
48. Zheng, J.; Huang, J.; Tao, L.; Li, Z.; Wang, Q. A Multifaceted Kinetic Model for the Thermal Decomposition of Calcium Carbonate. *Crystals* **2020**, *10*, 849. [[CrossRef](#)]
49. Reeder, R.J. Crystal chemistry of the rhombohedral carbonates. *Rev. Mineralogy.* **1983**, *11*, 1–47.
50. Bater, G. Thermal expansion anisotropy of dolomite-type borates Me₂ + Me₄ + B₂O₆. *Z. Krist. Cryst. Mater.* **1971**, *133*, 85–90. [[CrossRef](#)]
51. Barber, D.J.; Heard, H.C.; Wenk, H.R. Deformation of dolomite single crystals from 20–800 °C. *Phys. Chem. Miner.* **1981**, *7*, 271–286. [[CrossRef](#)]
52. Reeder, R.J.; Markgraf, S.A. High-temperature crystal chemistry of dolomite. *Am. Mineral.* **1986**, *71*, 795–804.
53. Robinson, K.; Gibbs, G.V.; Ribbe, P.H. Quadratic elongation: A quantitative measure of distortion in coordination polyhedra. *Science* **1971**, *172*, 567–570. [[CrossRef](#)]
54. Markgraf, S.A.; Reeder, R.J. High-temperature structure refinements of calcite and magnesite. *Am. Mineral.* **1985**, *70*, 590–600.
55. Hazen, R.M.; Prewitt, C.T. Effects of temperature and pressure on interatomic distances in oxygen-based minerals. *Am. Mineral.* **1977**, *62*, 309–315.
56. Hazen, R.M.; Finger, L.W. *Comparative Crystal Chemistry*; John Wiley: New York, NY, USA, 1982.
57. Sygała, A.; Bukowska, M.; Janoszek, T. High temperature versus geomechanical parameters of selected rocks—the present state of research. *J. Sustain. Min.* **2013**, *12*, 45–51. [[CrossRef](#)]
58. Wu, G.; Wang, Y.; Swift, G.; Chen, J. Laboratory investigation of the effects of temperature on the mechanical properties of sandstone. *Geotech. Geol. Eng.* **2013**, *31*, 809–816. [[CrossRef](#)]
59. Coppola, M.; Correale, A.; Barberio, M.D.; Billi, A.; Cavallo, A.; Fondriest, M.; Nazzari, M.; Paonita, A.; Romano, C.; Stagno, V.; et al. Meso-to nano-scale evidence of fluid-assisted co-seismic slip along the normal Mt. Morrone Fault, Italy: Implications for earthquake hydrogeochemical precursors. *Earth Planet. Sci. Lett.* **2021**, *568*, 117010. [[CrossRef](#)]
60. Zhi-jun, W.; Yang-Sheng, Z.; Yuan, Z.; Chong, W. Research status quo and prospection of mechanical characteristics of rock under high temperature and high pressure. *Procedia Earth Planet. Sci.* **2009**, *1*, 565–570.
61. Małkowski, P.; Skrzypkowski, K.; Bożęcki, P. Zmiany zachowania się skał pod wpływem wysokich temperatur w rejonie georeaktora. *Pr. Nauk. GIG Górnictwo Środowisko* **2011**, *4*, 259–272.
62. Małkowski, P.; Kamiński, P.; Skrzypkowski, K. Impact of Heating of carboniferous rocks on their mechanical parameters. *AGH J. Min. Geengin.* **2012**, *36*, 231–242.
63. Ranjith, P.G.; Viète, D.R.; Chen, B.J.; Perera, M.S.A. Transformation plasticity and the effect of temperature on the mechanical behavior of Hawkesbury sandstone at atmospheric pressure. *Eng. Geol.* **2012**, *151*, 120–127.

64. Chen, L.J.; Jun, H.E.; Chao, J.Q.; Qin, B.D. Swelling and breaking characteristics of limestone under high temperatures. *Min. Sci. Technol.* **2009**, *19*, 503–507. [[CrossRef](#)]
65. Sivrikaya, O. A study on the physicochemical and thermal characterization of dolomite and limestone samples for use in ironmaking and steelmaking. *Ironmak. Steelmak.* **2018**, *45*, 764–772. [[CrossRef](#)]
66. Zhang, W.; Sun, Q. Identification of primary mineral elements and macroscopic parameters in thermal damage process of limestone with canonical correlation analysis. *Rock Mech. Rock Eng.* **2018**, *51*, 1287–1292. [[CrossRef](#)]
67. Meng, Q.B.; Wang, C.K.; Liu, J.F.; Zhang, M.W.; Lu, M.M.; Wu, Y. Physical and microstructural characteristics of limestone after high-temperature exposure. *Bull. Eng. Geol. Environ.* **2020**, *79*, 1259–1274. [[CrossRef](#)]
68. Paterson, M.S.; Wong, T.F. *Experimental Rock Deformation—The Brittle Field*; Springer Science & Business Media: Berlin/Heidelberg, Germany, 2005.
69. Hoek, E.; Martin, C.D. Fracture initiation and propagation in intact rock—A review. *J. Rock Mech. Geotech. Eng.* **2014**, *6*, 287–300. [[CrossRef](#)]
70. Fredrich, J.T.; Evans, B.; Wong, T.F. Effect of grain size on brittle and semi brittle strength: Implications for micromechanical modeling of failure in compression. *J. Geophys. Res. Solid Earth* **1990**, *95*, 10907–10920. [[CrossRef](#)]
71. Hoagland, R.G.; Hahn, G.T.; Rosenfield, A.R. Influence of microstructure on fracture propagation in rock. *Rock Mech.* **1973**, *5*, 77–106. [[CrossRef](#)]
72. Holm, P.E. Effects of temperature and strain rate on the experimental deformation of an early-cemented Jurassic Limestone. *J. Geol.* **1983**, *91*, 714–719. [[CrossRef](#)]
73. Vajdova, V.; Zhu, W.; Chen, T.M.N.; Wong, T.F. Micromechanics of brittle faulting and cataclastic flow in Tavel limestone. *J. Struct. Geol.* **2010**, *32*, 1158–1169. [[CrossRef](#)]
74. De Bresser, J.H.P.; Spiers, C.J. Strength characteristics of the r, f, and c slip systems in calcite. *Tectonophysics* **1997**, *272*, 1–23. [[CrossRef](#)]
75. Schmid, S.M.; Boland, J.N.; Paterson, M.S. Superplastic flow in fine-grained limestone. *Tectonophysics* **1977**, *43*, 257–291. [[CrossRef](#)]
76. Li, W.; An, X.; Li, H. Limestone mechanical deformation behavior and failure mechanisms: A review. *Acta Geochim.* **2018**, *37*, 153–170. [[CrossRef](#)]
77. Luo, Z.Y.; Jin, Z.M. Superplastic deformation of rocks and its dynamic implication. *Geol. Sci. Technol. Inf.* **2003**, *22*, 17–23.
78. Myer, L.R.; Kemeny, J.M.; Zheng, Z.; Suarez, R.; Ewy, R.T.; Cook, N.G.W. Extensile cracking in the porous rock under differential compressive stress. *Appl. Mech. Rev.* **1992**, *45*, 263–280. [[CrossRef](#)]
79. Zhao, W.; Cao, P. *Rock Mechanics*; Central South University Press: Chang Sha, China, 2013; pp. 15–17.
80. Mao, X.B.; Zhang, L.Y.; Li, T.Z.; Liu, H.S. Properties of failure mode and thermal damage for limestone at high temperature. *Min. Sci. Technol.* **2009**, *19*, 290–294. [[CrossRef](#)]
81. Castagna, A.; Ougier-Simonin, A.; Benson, P.M.; Browning, J.; Walker, R.J.; Fazio, M.; Vinciguerra, S. Thermal damage and pore pressure effects of the Brittle-Ductile transition in comiso limestone. *J. Geophys. Res. Solid Earth* **2018**, *123*, 7644–7660. [[CrossRef](#)]
82. Zhang, L.; Mao, X.; Lu, A. Experimental study on the mechanical properties of rocks at high temperature. *Sci. China Ser. E Technol. Sci.* **2009**, *52*, 641–646. [[CrossRef](#)]
83. Brotons, V.; Tomás, R.; Ivorra, S.; Alarcón, J.C. Temperature influence on the physical and mechanical properties of a porous rock: San Julian’s calcarenite. *Eng. Geol.* **2013**, *167*, 117–127. [[CrossRef](#)]
84. Zhang, W.; Sun, Q.; Hao, S.; Wang, B. Experimental study on the thermal damage characteristics of limestone and the underlying mechanism. *Rock Mech. Rock Eng.* **2016**, *49*, 2999–3008. [[CrossRef](#)]
85. Kramer, S.L. *Geotechnical Earthquake Engineering*; Prentice Hall: Upper Saddle River, NJ, USA, 1996.
86. Zhang, Q. *Mechanical Behavior of Rock Materials under Dynamic Loading (No. THESIS)*; EPFL: Lausanne, Switzerland, 2014.
87. Waqas, U.; Ahmed, M.F.; Rogers, J.D. Effect of loading frequencies on the dynamic properties of thermally treated rock samples. In *52nd US Rock Mechanics/Geomechanics Symposium*; American Rock Mechanics Association: Alexandria, VA, USA, 2018.
88. Johansson, E.; Rautakorpi, J. *Rock Mechanics Stability at Olkiluoto, Hästholmen, Kivetty and Romuvaara (No. POSIVA-00-02)*; Posiva Oy: Eurajoki, Finland, 2000.
89. Ping, Q.; Zhang, C.; Su, H.; Zhang, H. Experimental Study on Dynamic Mechanical Properties and Energy Evolution Characteristics of Limestone Specimens Subjected to High Temperature. *Adv. Civ. Eng.* **2020**, *2020*, 8875568. [[CrossRef](#)]
90. Ahmed, M.F.; Waqas, U.; Arshad, M.; Rogers, J.D. Effect of heat treatment on dynamic properties of selected rock types taken from the Salt Range in Pakistan. *Arab. J. Geosci.* **2018**, *11*, 728. [[CrossRef](#)]
91. Yu, L.; Su, H.; Liu, R.; Jing, H.; Li, G.; Li, M. Effect of Thermal Treatment on the Dynamic Behaviors at a Fixed Loading Rate of Limestone in Quasi-vacuum and Air-filled Environments. *Lat. Am. J. Solids Struct.* **2018**, *15*, 15. [[CrossRef](#)]
92. Crosby, Z.K. *Effects of Thermally Induced Microcracking on the Quasi-Static and Dynamic Response of Salem Limestone (No. ERDC/GSL TR-17-15)*; US Army Engineer Research and Development Center, Geotechnical and Structures Laboratory Vicksburg United States: Vicksburg, MS, USA, 2017.
93. Zou, F.; Fang, Z.F.; Xia, M.Y. Study on Dynamic Mechanical Properties of Limestone under Uniaxial Impact Compressive Loads. *Math. Probl. Eng.* **2016**, *2016*, 5207457. [[CrossRef](#)]
94. Zhou, Y.X.; Xia, K.W.; Li, X.B.; Li, H.B.; Ma, G.W.; Zhao, J.; Zhou, Z.L.; Dai, F. Suggested methods for determining the dynamic strength parameters and mode-I fracture toughness of rock materials. In *The ISRM Suggested Methods for Rock Characterization, Testing, and Monitoring: 2007–2014*; Springer: Cham, Switzerland, 2011; pp. 35–44.

95. Yuan, F.; Prakash, V. Use of a modified torsional Kolsky bar to study frictional slip resistance in rock-analog materials at coseismic slip rates. *Int. J. Solids Struct.* **2008**, *45*, 4247–4263. [[CrossRef](#)]
96. Wang, Q.Z.; Li, W.; Song, X.L. A method for testing dynamic tensile strength and elastic modulus of rock materials using SHPB. *Pure Appl. Geophys.* **2006**, *163*, 1091–1100. [[CrossRef](#)]
97. Zhao, H.; Gary, G. On the use of SHPB techniques to determine the dynamic behavior of materials in the range of small strains. *Int. J. Solids Struct.* **1996**, *33*, 3363–3375. [[CrossRef](#)]
98. Lindholm, U.S.; Yeakley, L.M.; Nagy, A. The dynamic strength and fracture properties of dresser basalt. *Int. J. Rock Mech. Min. Sci. Geomech. Abstr.* **1974**, *11*, 181–191. [[CrossRef](#)]
99. Kumar, A. The effect of stress rate and temperature on the strength of basalt and granite. *Geophysics* **1968**, *33*, 501–510. [[CrossRef](#)]
100. Kolesnikov, Y.I. Dispersion effect of velocities on the evaluation of material elasticity. *J. Min. Sci.* **2009**, *45*, 347. [[CrossRef](#)]
101. Zhang, Q.B.; Zhao, J. A review of dynamic experimental techniques and mechanical behavior of rock materials. *Rock Mech. Rock Eng.* **2014**, *47*, 1411–1478. [[CrossRef](#)]
102. Fjær, E. Relations between static and dynamic moduli of sedimentary rocks. *Geophys. Prospect.* **2019**, *67*, 128–139. [[CrossRef](#)]
103. Regnet, J.B.; David, C.; Robion, P.; Menéndez, B. Microstructures and physical properties in carbonate rocks: A comprehensive review. *Mar. Pet. Geol.* **2019**, *103*, 366–376. [[CrossRef](#)]
104. Lucia, F.J. *Carbonate Reservoir Characterization: An Integrated Approach*; Springer Science & Business Media: Berlin/Heidelberg, Germany, 2007.
105. Bisai, R.; Palaniappan, S.K.; Pal, S.K. Effects of high-temperature heating and cryogenic quenching on the physico-mechanical properties of limestone. *SN Appl. Sci.* **2020**, *2*, 158. [[CrossRef](#)]
106. Liu, J.; Li, B.; Tian, W.; Wu, X. Investigating and predicting permeability variation in thermally cracked dry rocks. *Int. J. Rock Mech. Min. Sci.* **2018**, *103*, 77–88. [[CrossRef](#)]
107. Trippetta, F.; Carpenter, B.M.; Mollo, S.; Scuderi, M.M.; Scarlato, P.; Collettini, C. Physical and transport property variations within carbonate-bearing fault zones: Insights from the Monte Maggio Fault (central Italy). *Geochem. Geophys. Geosyst.* **2017**, *18*, 4027–4042. [[CrossRef](#)]
108. Berryman, J.G.; Wang, H.F. Elastic wave propagation and attenuation in a double-porosity dual-permeability medium. *Int. J. Rock Mech. Min. Sci.* **2000**, *37*, 63–78. [[CrossRef](#)]
109. Dvorkin, J.; Nur, A.; Yin, H. Effective properties of cemented granular materials. *Mech. Mater.* **1994**, *18*, 351–366. [[CrossRef](#)]
110. Walton, K. The effective elastic moduli of a random packing of spheres. *J. Mech. Phys. Solids* **1987**, *35*, 213–226. [[CrossRef](#)]
111. Berryman, J.G. Long-wavelength propagation in composite elastic media II. Ellipsoidal inclusions. *J. Acoust. Soc. Am.* **1980**, *68*, 1820–1831. [[CrossRef](#)]
112. Bagrintseva, K.I. *Conditions of Generation and Properties of Carbonate Reservoirs of Oil and Gas*; RGGU: Moscow, Russia, 1999. (In Russian)
113. Zinszner, B.; Pellerin, F.M. *A Geoscientist's Guide to Petrophysics*; Editions Technip: Paris, France, 2007; p. 384.
114. Mukerji, T.; Dvorkin, J. *The Rock Physics Handbook*, 2nd ed.; Cambridge University Press: Cambridge, UK, 2009.
115. Homand-Etienne, F.; Troalen, J.P. Behaviour of granites and limestones subjected to slow and homogeneous temperature changes. *Eng. Geol.* **1984**, *20*, 219–233. [[CrossRef](#)]
116. Lion, M.; Skoczylas, F.; Ledésert, B. Effects of heating on the hydraulic and poroelastic properties of Bourgogne limestone. *Int. J. Rock Mech. Min. Sci.* **2005**, *42*, 508–520. [[CrossRef](#)]
117. Heap, M.J.; Mollo, S.; Vinciguerra, S.; Lavallée, Y.; Hess, K.U.; Dingwell, D.B.; Baud, P.; Iezzi, G. Thermal weakening of the carbonate basement under Mt. Etna volcano (Italy): Implications for volcano instability. *J. Volcanol. Geotherm. Res.* **2013**, *250*, 42–60. [[CrossRef](#)]
118. Li, F.B.; Sheng, J.C.; Zhan, M.L.; Xu, L.M.; Qiang Wu Jia, C.L. Evolution of limestone fracture permeability under coupled thermal, hydrological, mechanical, and chemical conditions. *J. Hydrodyn. Ser. B* **2014**, *26*, 234–241. [[CrossRef](#)]
119. Min, S.H.; Jianfeng, S.H.; Anjiang, S.H.; Liyin, P.A.; Anping, H.U.; Yuanyuan, H.U. Experimental simulation of dissolution law and porosity evolution of carbonate rock. *Pet. Explor. Dev.* **2016**, *43*, 616–625.
120. Timoshenko, S.P.; Goodier, J.N. Two-dimensional problems in polar coordinates. In *Theory of Elasticity*, 3rd ed.; McGraw-Hill: New York, NY, USA, 1970; pp. 65–149.
121. Çanakci, H.; Demirboğa, R.; Karakoç, M.B.; Şirin, O. Thermal conductivity of limestone from Gaziantep (Turkey). *Build. Environ.* **2007**, *42*, 1777–1782. [[CrossRef](#)]
122. Demirboğa, R. Influence of mineral admixtures on thermal conductivity and compressive strength of mortar. *Energy Build.* **2003**, *35*, 189–192. [[CrossRef](#)]
123. Robertson, E.C. Thermal Properties of Rocks. 1988. Available online: <https://pubs.usgs.gov/of/1988/0441/report.pdf> (accessed on 1 March 2022).
124. Lo, K.Y.; Wai, R.S.C. Thermal expansion, diffusivity, and cracking of rock cores from Darlington, Ontario. *Can. Geotech. J.* **1982**, *19*, 154–166. [[CrossRef](#)]
125. Hanley, E.J.; Dewitt, D.P.; Roy, R.F. The thermal diffusivity of eight well-characterized rocks for the temperature range 300–1000 K. *Eng. Geol.* **1978**, *12*, 31–47. [[CrossRef](#)]
126. Freeman, D.C.; Sawdye, J.A.; Mumpton, F.A. The mechanism of thermal spalling in rocks. *Colo. Sch. Mines Q.* **1963**, *58*, 225–252.
127. Clark, S.P. (Ed.) *Handbook of Physical Constants*; Memoir-Geological Society of America: New York, NY, USA, 1966; Volume 97.

128. Wong, T.F.; Brace, W.F. Thermal expansion of rocks: Some measurements at high pressure. *Tectonophysics* **1979**, *57*, 95–117. [[CrossRef](#)]
129. Pertermann, M.; Whittington, A.G.; Hofmeister, A.M.; Spera, F.J.; Zayak, J. Transport properties of low-sanidine single-crystals, glasses and melts at high temperature. *Contrib. Mineral. Petrol.* **2008**, *155*, 689–702. [[CrossRef](#)]
130. Hofmeister, A.M. Thermal diffusivity of garnets at high temperature. *Phys. Chem. Miner.* **2006**, *33*, 45–62. [[CrossRef](#)]
131. Popov, Y.A.; Pribnow, D.F.; Sass, J.H.; Williams, C.F.; Burkhardt, H. Characterization of rock thermal conductivity by high-resolution optical scanning. *Geothermics* **1999**, *28*, 253–276. [[CrossRef](#)]
132. Degiovanni, A.; Andre, S.; Maillet, D. Phonic conductivity measurement of a semi-transparent material. *Therm. Conduct.* **1993**, *22*, 623.
133. Fei, Y. *Thermal Expansion, Mineral Physics and Crystallography: A Handbook of Physical Constants*; AUG: Washington, DC, USA, 1995; Volume 2, pp. 29–44.
134. Shen, Y.; Yang, Y.; Yang, G.; Hou, X.; Ye, W.; You, Z.; Xi, J. Damage characteristics and thermo-physical properties changes of limestone and sandstone during thermal treatment from -30°C to 1000°C . *Heat Mass Transf.* **2018**, *54*, 3389–3407. [[CrossRef](#)]
135. Miao, S.; Zhou, Y. Temperature dependence of thermal diffusivity and conductivity for sandstone and carbonate rocks. *J. Therm. Anal. Calorim.* **2018**, *131*, 1647–1652. [[CrossRef](#)]
136. Khan, L.A.; Maqsood, A. Prediction of effective thermal conductivity of porous consolidated media as a function of temperature: A test example of limestones. *J. Phys. D Appl. Phys.* **2007**, *40*, 4953.
137. Vosteen, H.D.; Schellschmidt, R. Influence of temperature on thermal conductivity, thermal capacity, and thermal diffusivity for different types of rock. *Phys. Chem. Earth Parts A/B/C* **2003**, *28*, 499–509. [[CrossRef](#)]
138. Mirkovich, V.V. Experimental study relating thermal conductivity to the thermal piercing of rocks. *Int. J. Rock Mech. Min. Sci. Geomech. Abstr.* **1968**, *5*, 205–218. [[CrossRef](#)]
139. Birch, A.F.; Clark, H. The thermal conductivity of rocks and its dependence upon temperature and composition. *Am. J. Sci.* **1940**, *238*, 529–558. [[CrossRef](#)]